

CONFIDENTIAL NASA TM X-124



063-12556
code-1
554205
32P

TECHNICAL MEMORANDUM

X-124

INVESTIGATION OF THE STATIC LONGITUDINAL STABILITY AND
ROLL CHARACTERISTICS OF A THREE-STAGE MISSILE
CONFIGURATION AT MACH NUMBERS

FROM 1.77 TO 2.87

By Donald T. Gregory and Ausley B. Carraway

Langley Research Center
Langley Field, Va.

CLASSIFICATION CHANGED TO
UNCLASSIFIED
THORITY NASA LIST #1, DEC 1, 1962

CLASSIFIED DOCUMENT - TITLE UNCLASSIFIED

This material contains information affecting the national defense of the United States within the meaning of the espionage laws, Title 18, U.S.C., Secs. 793 and 794, the transmission or revelation of which in any manner to an unauthorized person is prohibited by law.

NATIONAL AERONAUTICS AND SPACE ADMINISTRATION
WASHINGTON

October 1959

CONFIDENTIAL

UNCLASSIFIED
CONFIDENTIAL

NATIONAL AERONAUTICS AND SPACE ADMINISTRATION

TECHNICAL MEMORANDUM X-124

INVESTIGATION OF THE STATIC LONGITUDINAL STABILITY AND

ROLL CHARACTERISTICS OF A THREE-STAGE MISSILE

CONFIGURATION AT MACH NUMBERS

FROM 1.77 TO 2.87*

By Donald T. Gregory and Ausley B. Carraway

SUMMARY

An investigation has been conducted in the Langley Unitary Plan wind tunnel to determine the static longitudinal stability characteristics of a three-stage missile configuration. Included in this investigation is the determination of effect of body deflection between missile stages and the effectiveness of fin cant angle in producing roll.

Tests were performed through an angle-of-attack range from -8° to 4° at Mach numbers of 1.77, 2.16, 2.54, and 2.87. The corresponding Reynolds numbers (based on model length) were 24.9×10^6 , 21.9×10^6 , 17.7×10^6 , and 20.1×10^6 .

The results show that the missile is longitudinally stable throughout the test Mach number and angle-of-attack range. Body deflection of as much as 1° between stages has little or no effect on the longitudinal stability characteristics. The rolling moment produced by the front fins is ineffective when rear fins are in place.

INTRODUCTION

The Langley Research Center of NASA has initiated a research program to detect, by radar, objects reentering the atmosphere at hypersonic speeds. The vehicle selected consists of four stages, of which the first three stages are used to obtain altitude and the fourth stage is used to accelerate a reentry configuration earthward at hypersonic speeds. One of the prerequisites of such a program is to determine the stability of the

*Title, Unclassified.

CONFIDENTIAL

CONFIDENTIAL

various stages in order that the configuration can be boosted and then projected earthward successfully. In order to expedite determination of the stability characteristics of the configuration, several facilities of the Langley Research Center have collaborated to test various stages of the configuration.

The data presented herein are results of tests on a scale model of the combined second, third, and fourth stages in the Langley Unitary Plan wind tunnel. The effect of canting the fins and relative roll alinement of the second and third stages, as well as deflection between the second and third and between the third and fourth stages, on the stability characteristics of the test configuration are included.

These results were obtained at Mach numbers of 1.77, 2.16, 2.54, and 2.87 through an angle-of-attack range from -8° to 4° for a sideslip angle of approximately 0° . The test Reynolds numbers (based on model length) for the Mach numbers of 1.77, 2.16, 2.54, and 2.87 are 24.9×10^6 , 21.9×10^6 , 17.7×10^6 , and 20.1×10^6 , respectively.

SYMBOLS

The coefficients of forces and moments presented are referred to the body axes system (fig. 1) with the origin at the center of gravity. (See fig. 2.) Symbols used in this paper are as follows:

C_A axial-force coefficient, $\frac{\text{Axial force}}{qS}$

$C_{A,c}$ chamber axial-force coefficient, $\frac{\text{Chamber axial force}}{qS}$

C_l rolling-moment coefficient, $\frac{\text{Rolling moment}}{qSl}$

C_m pitching-moment coefficient, $\frac{\text{Pitching moment}}{qSl}$

$$C_{m_\alpha} = \frac{\partial C_m}{\partial \alpha}$$

C_N normal-force coefficient, $\frac{\text{Normal force}}{qS}$

$$C_{N_\alpha} = \frac{\partial C_N}{\partial \alpha}$$

CONFIDENTIAL

l	model length, in.
M	free-stream Mach number
q	free-stream dynamic pressure, lb/sq ft
S	cross-sectional area of first-stage body, sq ft
α	angle of attack of model center line, deg

APPARATUS AND METHODS

Wind Tunnel

Tests were conducted in the low Mach number test section of the Langley Unitary Plan wind tunnel, which is a variable pressure, continuous-flow tunnel. The nozzle leading to the test section is of the asymmetric sliding-block type, which permits a continuous variation in test section Mach number from about 1.5 to 2.9.

Model

A two-view drawing with dimensional details of the model tested is presented as figure 2. Photographs of the model are presented as figure 3. The model configuration consisted of the remaining three stages of a four-stage missile configuration. For purposes of clarity, these combined second, third, and fourth stages are referred to as stages I, II, and III herein, stage III being the most forward stage of the configuration. The basic configuration combined the three stages with 0° body deflection and included interdigitated fins on stage I and stage II.

The configuration was designed in such a manner that stages I and II could be deflected 0.50° or 1.00° (stage II at positive angle of attack with respect to stage I) and stage II and stage III could be deflected 0.50° with respect to each other.

Stages I and II of the configuration were equipped with cruciform fins which could be placed so that either the rear fins (stage I) were in line or interdigitated with the front fins (stage II). In addition, two of the fins on each of these stages could be set at angles of cant relative to the center line. As a result of inaccuracy in construction of the model fins, the angular settings of the various fins were not symmetrical. Figure 4 shows the angular cant of each fin, and an average cant angle of each cruciform fin configuration tested. These average cant angles are herein referred to as effective cant angles.

Test Conditions

The test conditions were as follows:

Mach number	1.77	2.16	2.54	2.87
Stagnation temperature, °F	125	125	150	150
Stagnation dewpoint, °F	-30	-30	-30	-30
Stagnation pressure, lb/sq in. abs	26	27	28	38
Reynolds number	24.92×10^6	21.89×10^6	17.71×10^6	20.08×10^6

All configurations were tested through an angle-of-attack range from approximately -8° to 4° at a sideslip angle of approximately 0° . The model, for all tests, incorporated a fixed-transition strip 1 inch rearward of the nose. The strip, which was $1/32$ inch wide, was composed of 0.012-inch carborundum grains.

Measurements

Forces and moments were measured by means of a six-component strain-gage balance mounted within the model. The balance was, in turn, rigidly fastened to the sting support system.

Balance-chamber pressure was measured with a single static orifice located in the vicinity of the balance.

Schlieren photographs of each configuration were taken at all test Mach numbers and at various model attitudes and test conditions.

Corrections

The angles of attack have been corrected for test section flow angularity and for deflection of the balance and sting under load. The axial-force data presented herein have been adjusted to correspond to zero balance-chamber axial-force. Measured pressure gradients are sufficiently small to assure that model buoyancy effects are negligible.

Accuracy

The accuracy of the individual measured quantities, based on calibrations and repeatability of data, is estimated to be within the following limits:

C_N	± 0.050
C_A	± 0.006
$C_{A,c}$	± 0.001
C_m	± 0.002
C_l	± 0.001
α , deg	± 0.10
M	± 0.015

PRESENTATION OF RESULTS

The results of the investigation are presented in the following figures:

	Figures
Typical schlieren photographs of model tested	5
Variation of chamber axial-force coefficient with angle of attack	6
Effect of body deflection on aerodynamic characteristics in pitch; fins interdigitated	7
Summary of longitudinal stability characteristics of body deflection	8
Effect of relative fin alinement on aerodynamic characteristics in pitch	9
Effect of stage I fin cant on rolling-moment coefficient	10
Effect of stage II fin cant on rolling-moment coefficient	11

DISCUSSION

Longitudinal Characteristics

The data of figure 7 show that the basic three-stage configuration is longitudinally stable throughout the test Mach number and angle-of-attack range. Examination of figure 8 shows the usual decrease in

longitudinal stability and normal-force-curve slope with increase in Mach number.

Body deflection of the configuration, such that stages II and III are as much as 1° upward with respect to stage I, or a similar deflection of 0.50° each between stages I and II and between stages II and III, has little effect on the axial-force (fig. 7) or longitudinal stability characteristics (fig. 8) of the test configuration at the test Mach numbers and angles of attack.

Tests were also performed with the rear fins in line with the forward fins, and the results of these tests (fig. 9) are little different from the results obtained with the basic model (fins interdigitated) insofar as pitching-moment and normal-force coefficients are concerned. The axial-force coefficients of the inline fin configurations were somewhat lower in the angle-of-attack range between about $\pm 3^\circ$. The reason for this difference is probably associated with a change in interference effects of the front fins on the rear fins; however, in the absence of a detailed pressure survey over the rear fins, no definite conclusions can be given.

It may be noted from figure 9 that the rear fins contribute about half of the normal-force coefficient of the total configuration, and without these fins, the test configuration is longitudinally unstable throughout the test Mach number range.

Roll Characteristics

The rolling-moment coefficients produced by either the rear (stage I) or front (stage II) set of fins are, in general, only slightly changed by the relative roll alignment of the fins (figs. 10 and 11). An exception to this is at angles of attack of approximately -6° for Mach numbers below 2.5. In this case, the rear fins are more effective roll producers when the fins are interdigitated than when the fins are in line.

The results shown in figure 10 indicate that the roll effectiveness of the rear fins is essentially constant with angle of attack for the test Mach number and angle-of-attack range.

The roll effectiveness of the front fins in the absence of the rear fins may be seen in figure 11. With the presence of the rear fins, however, the rolling-moment coefficient per degree fin cant produced by the front fins is ineffective at all Mach numbers and angles of attack (fig. 11). Unpublished data indicate that this ineffectiveness is caused by downwash from these fins acting on the rear fins in a direction to counteract the rolling moment produced by these front fins.

UNCLASSIFIED

CONCLUSIONS

The results of an investigation of a three-stage missile configuration at Mach numbers of 1.77, 2.16, 2.54, and 2.87 at corresponding Reynolds numbers (based on model length) of 24.9×10^6 , 21.9×10^6 , 17.7×10^6 , and 20.1×10^6 , respectively, indicate the following conclusions:

1. The basic missile configuration is longitudinally stable throughout the test Mach number and angle-of-attack range.
2. Body deflection of as much as 1° between stages has little effect on the longitudinal stability characteristics.
3. The rolling moment produced by the front fins is ineffective when the rear fins are in place.

Langley Research Center,
National Aeronautics and Space Administration,
Langley Field, Va., July 17, 1959.

CONFIDENTIAL

CONFIDENTIAL

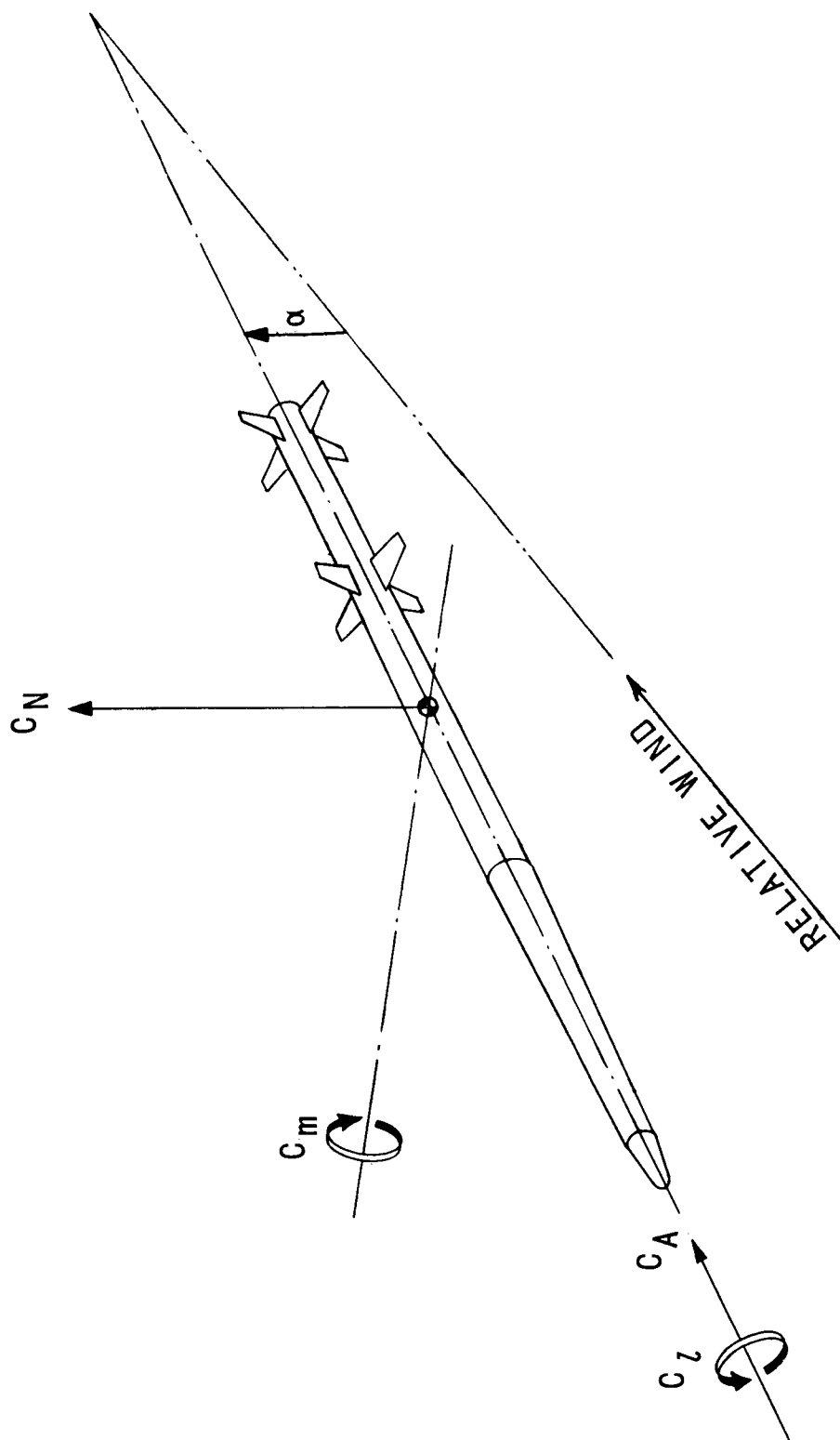


Figure 1.- Body axes system. (Arrows indicate positive directions.)

CONFIDENTIAL

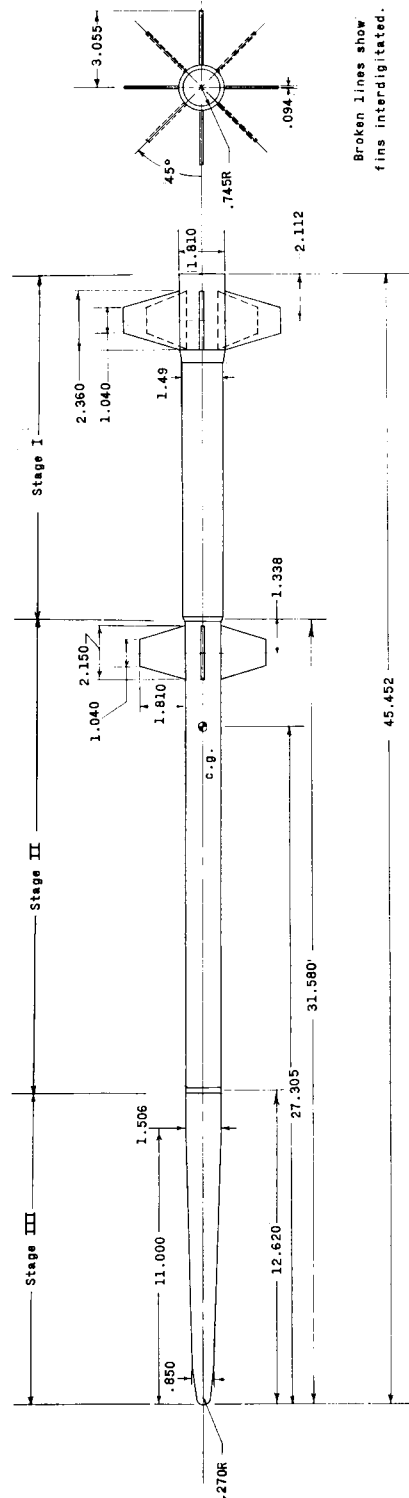
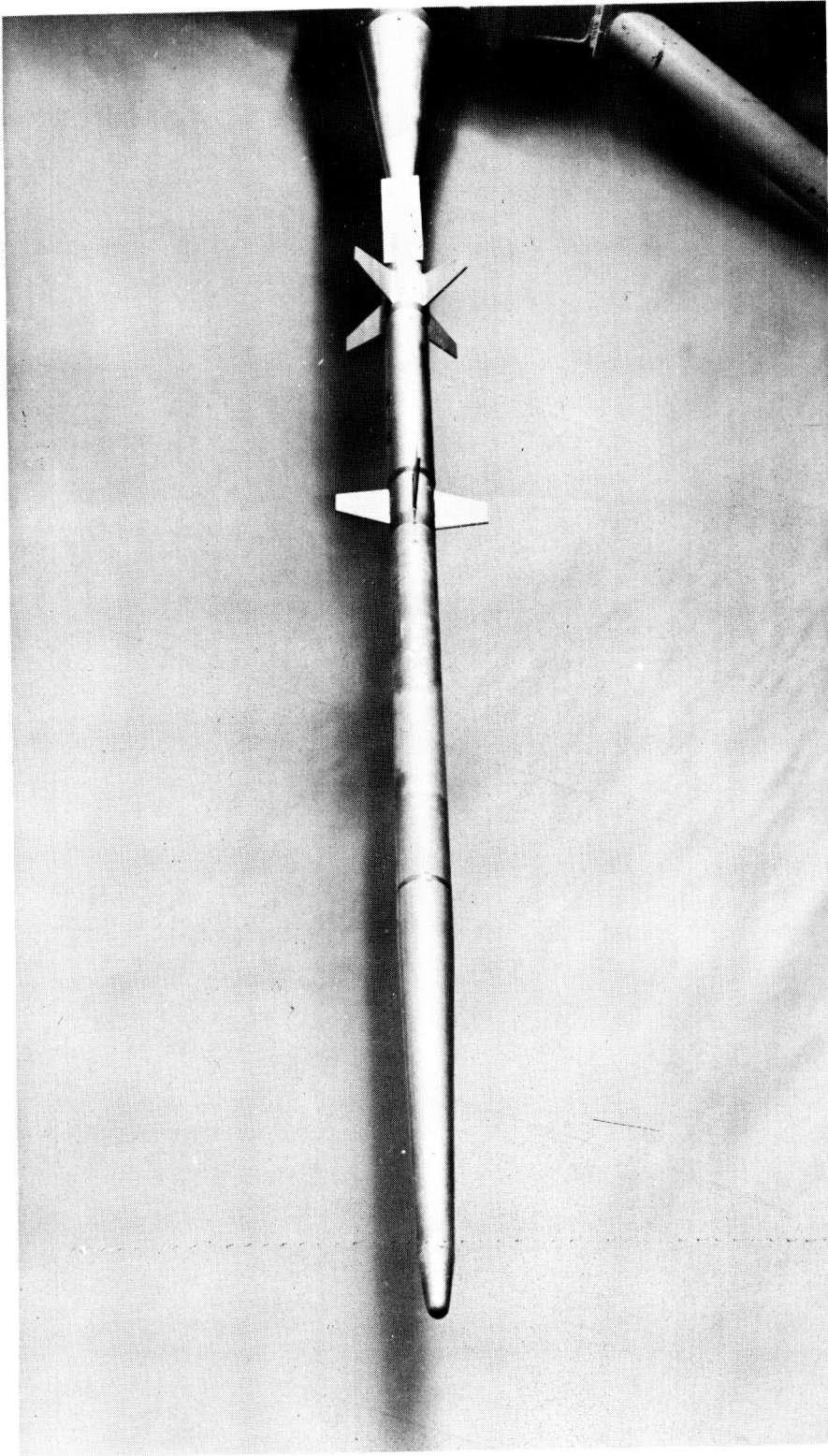
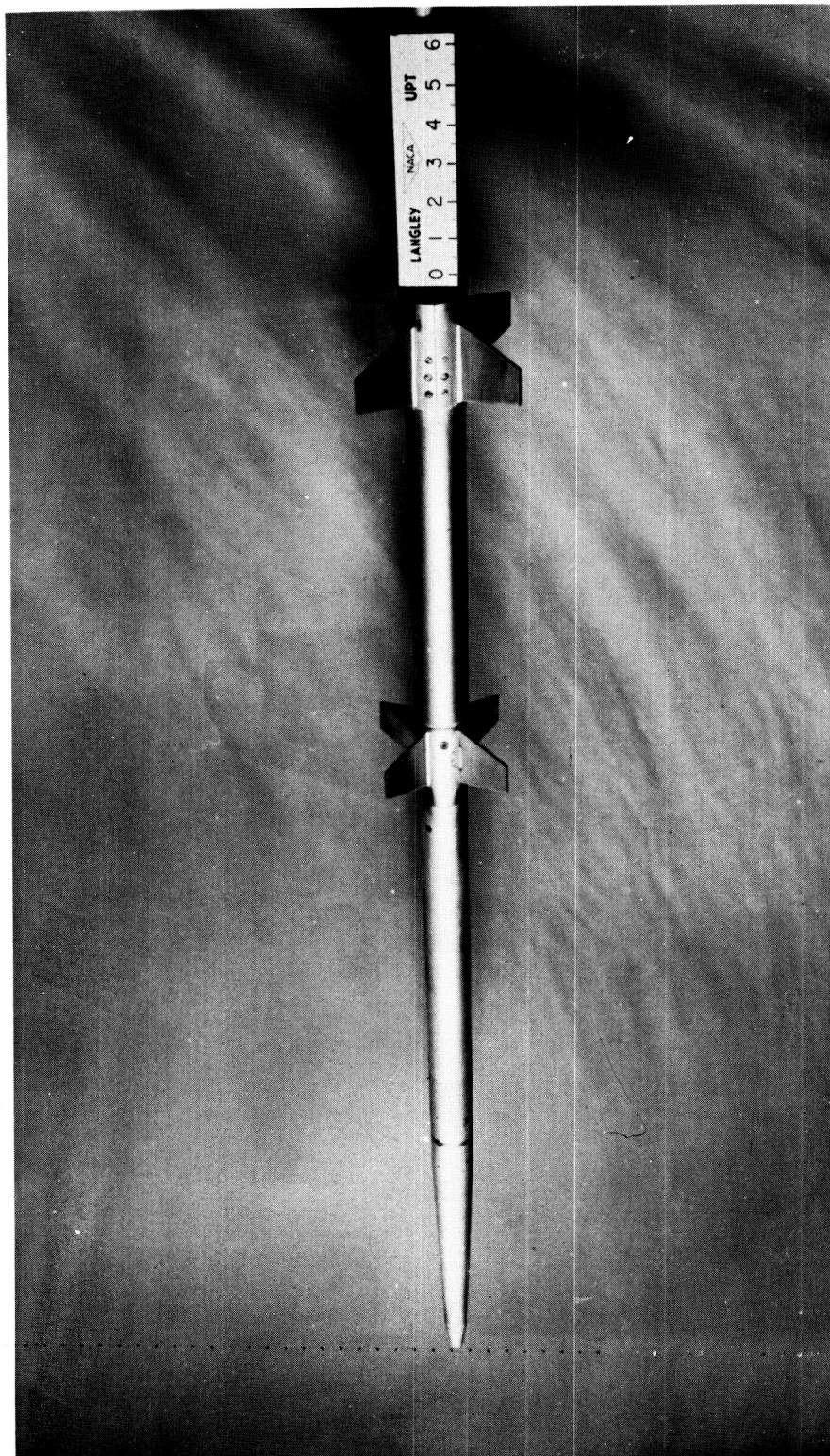


Figure 2.- Model details. All dimensions are in inches unless otherwise noted.



(a) Fins interdigitated; three-quarter front view. L-58-4024

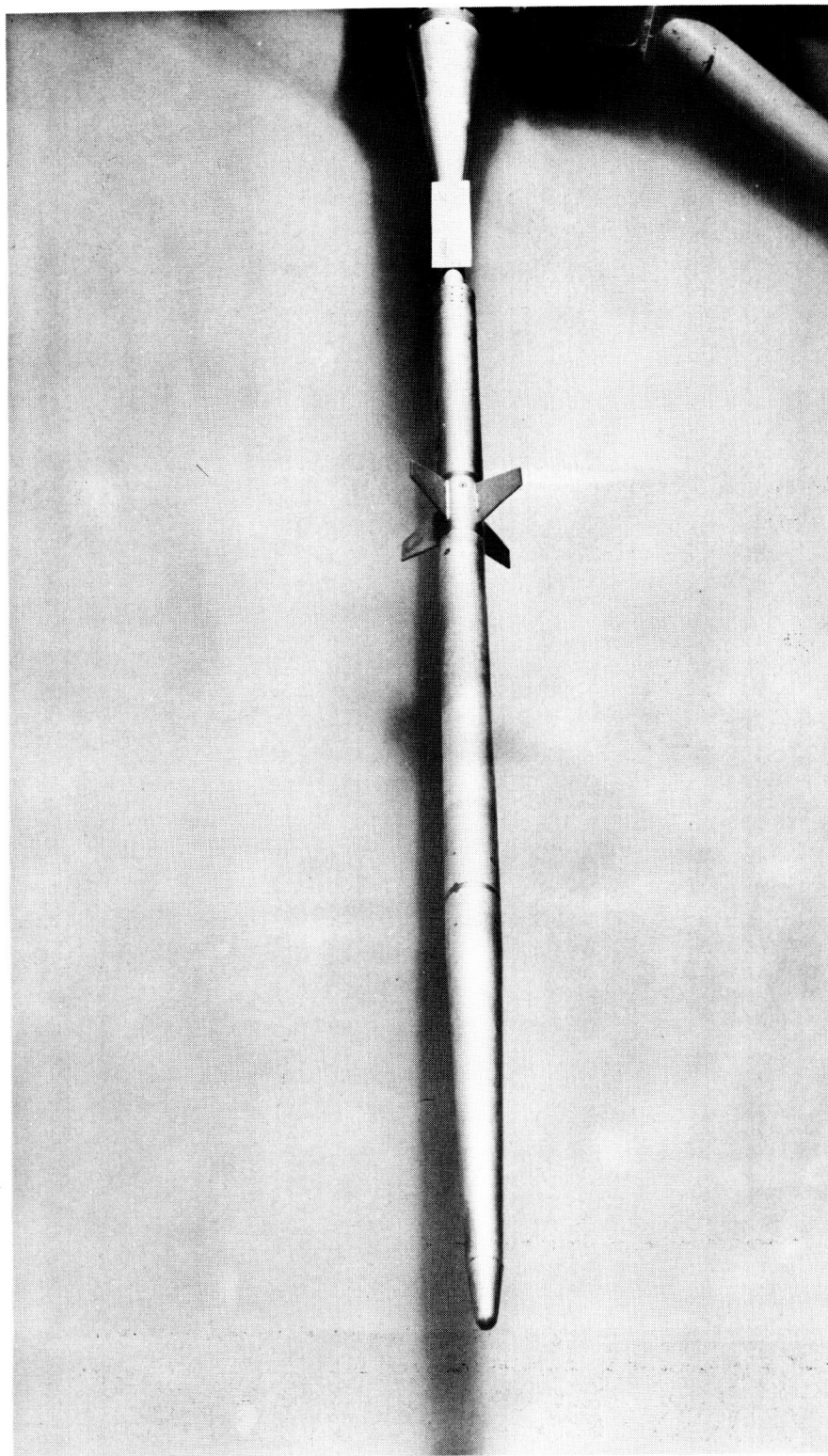
Figure 3.- Model photographs.



L-58-4027

(b) Fins in line; three-quarter rear view.

Figure 3.- Continued.

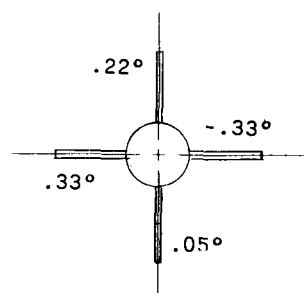
0317123010RU
CONFIDENTIAL

(c) Rear fins removed; three-quarter front view. L-58-4023

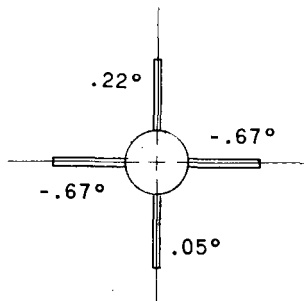
Figure 3.- Concluded.

CONFIDENTIAL

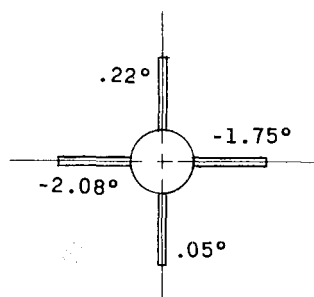
Stage II fins



Nominal setting 0°
Effective setting $.14^\circ$

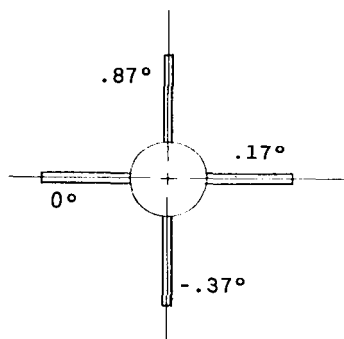


Nominal setting -1°
Effective setting $-.54^\circ$

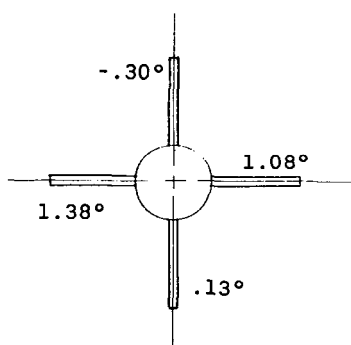


Nominal setting -2°
Effective setting -1.78°

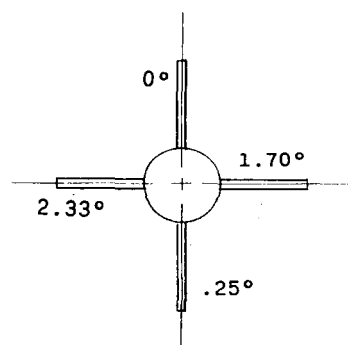
Stage I fins



Nominal setting 0°
Effective setting $.34^\circ$



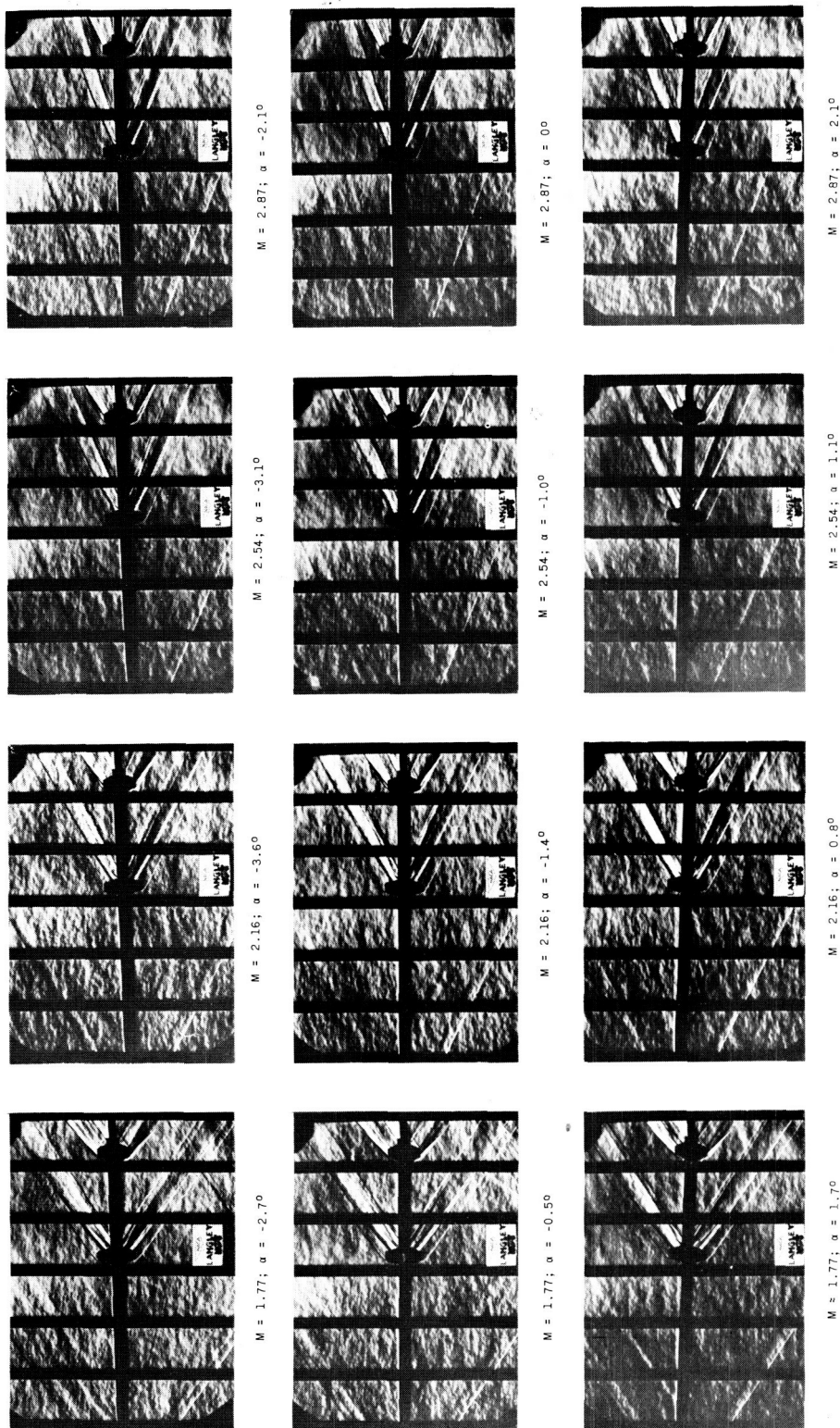
Nominal setting 1°
Effective setting 1.15°



Nominal setting 2°
Effective setting 2.14°

Figure 4.- Effective cant angles for each fin setting tested as viewed from rear.

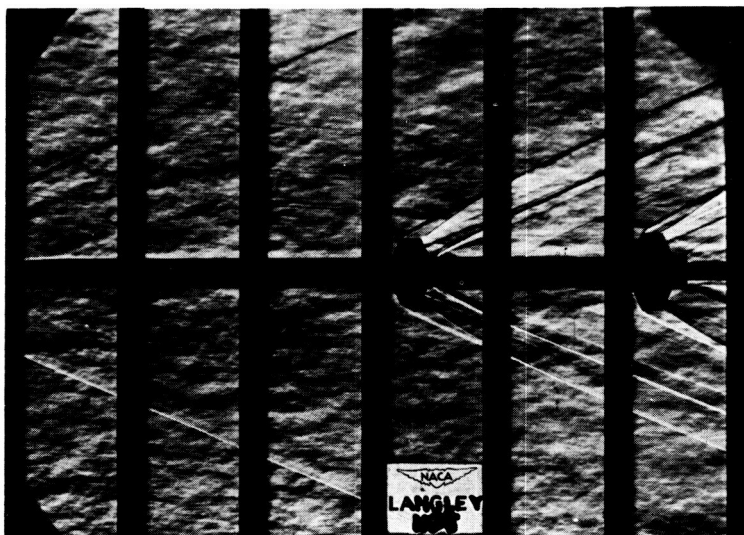
CONFIDENTIAL



(a) Fins interdigitated. L-59-5003

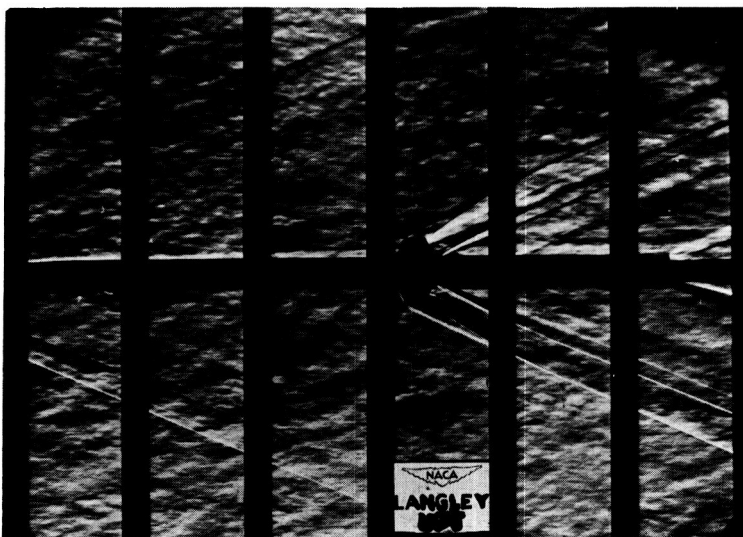
Figure 5.- Typical schlieren photographs of model tested.

CONFIDENTIAL



$M = 2.54; \alpha = -1.0^\circ$

(b) Fins in line.



$M = 2.54; \alpha = -1.0^\circ$

(c) Rear fins removed.

L-59-5004

Figure 5.- Concluded.

CONFIDENTIAL

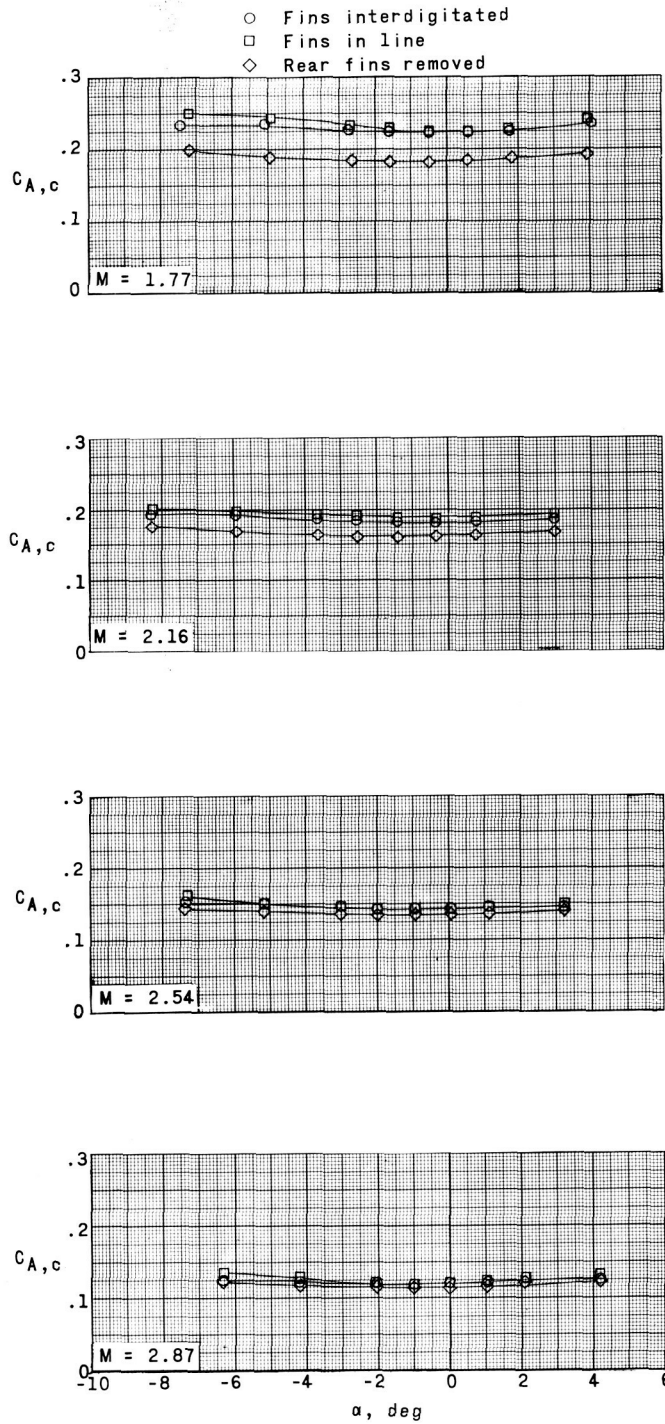
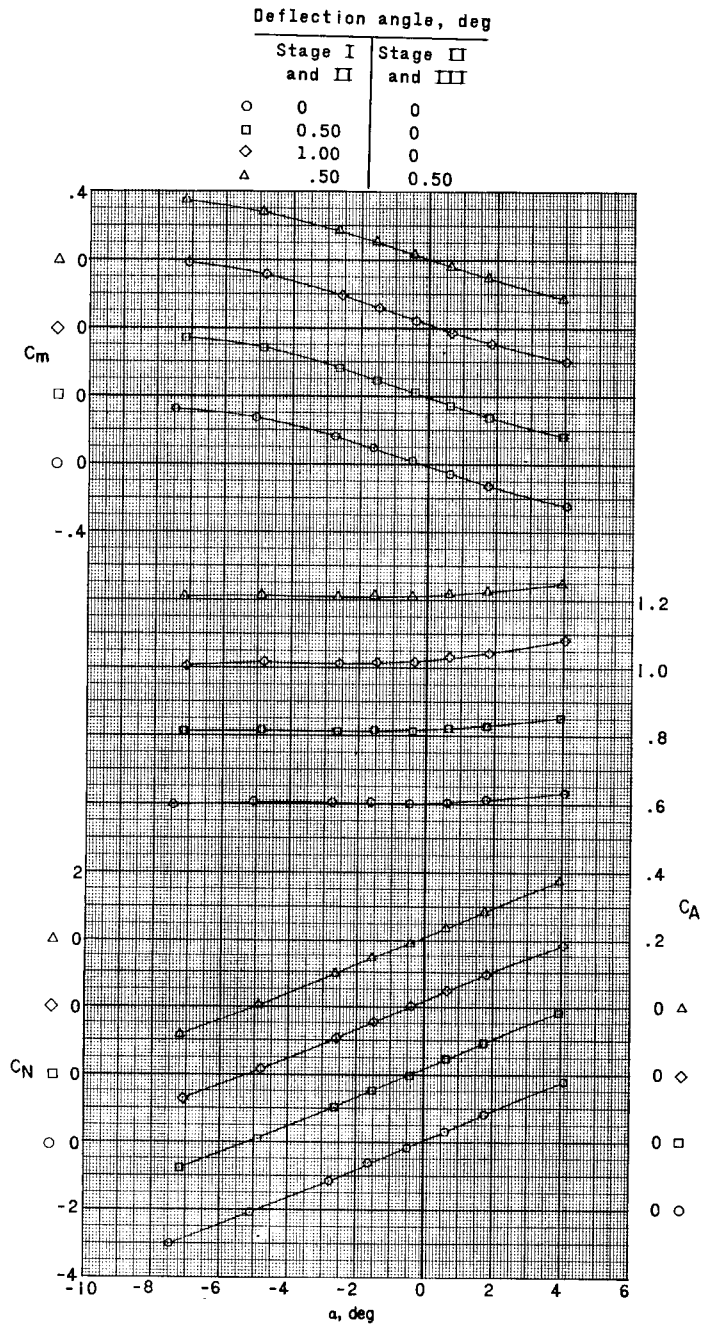


Figure 6.- Variation of chamber axial-force coefficient with angle of attack.

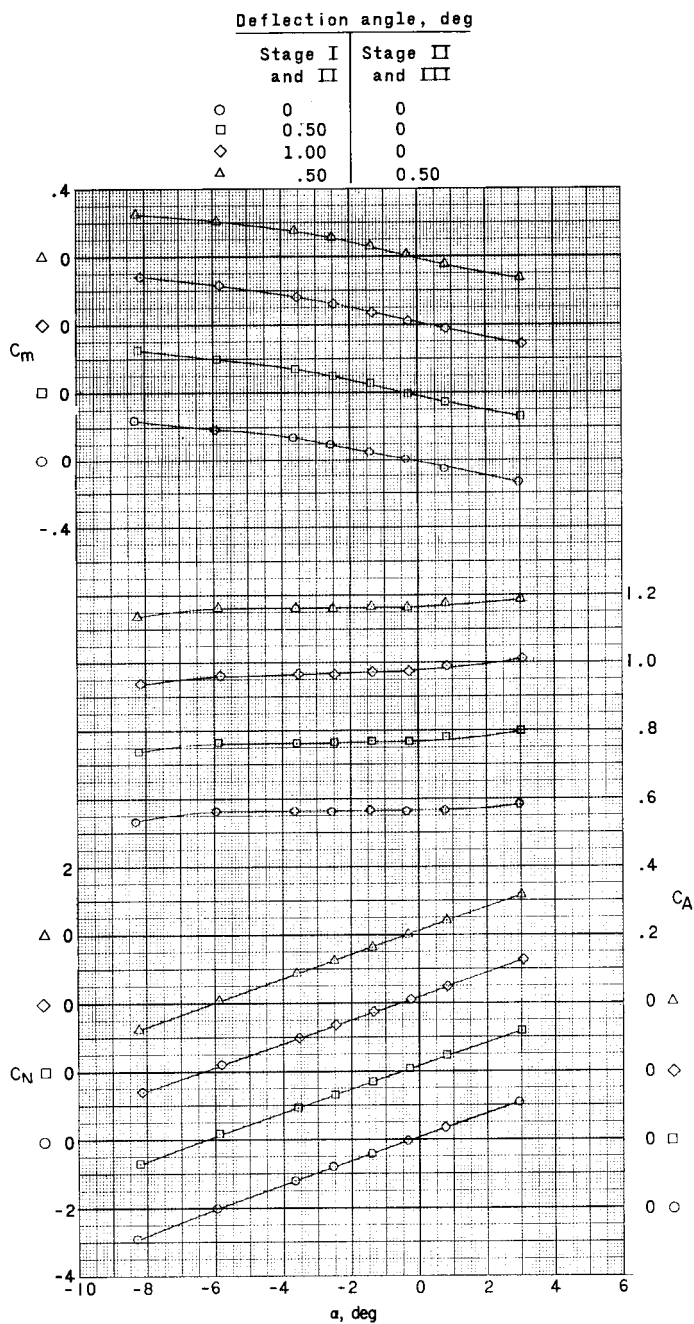
CONFIDENTIAL



(a) $M = 1.77$.

Figure 7.- Effect of body deflection on aerodynamic characteristics in pitch. Fins interdigitated.

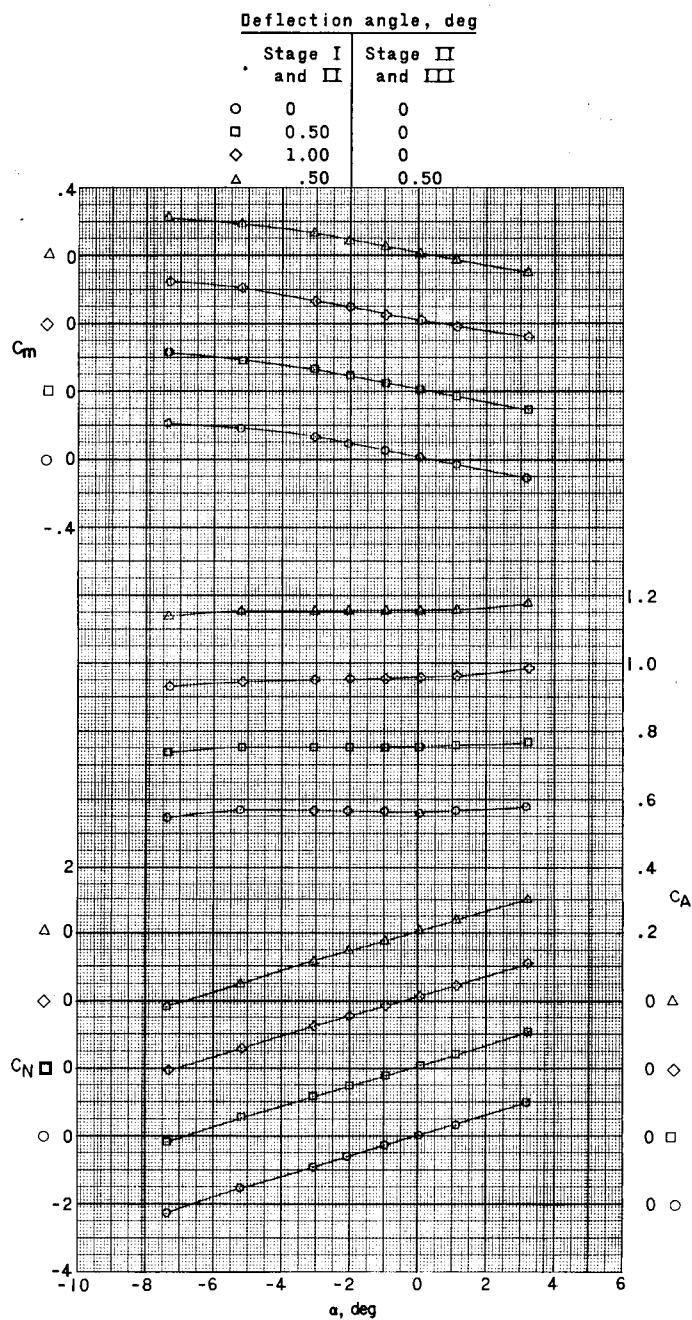
CONFIDENTIAL



(b) $M = 2.16$.

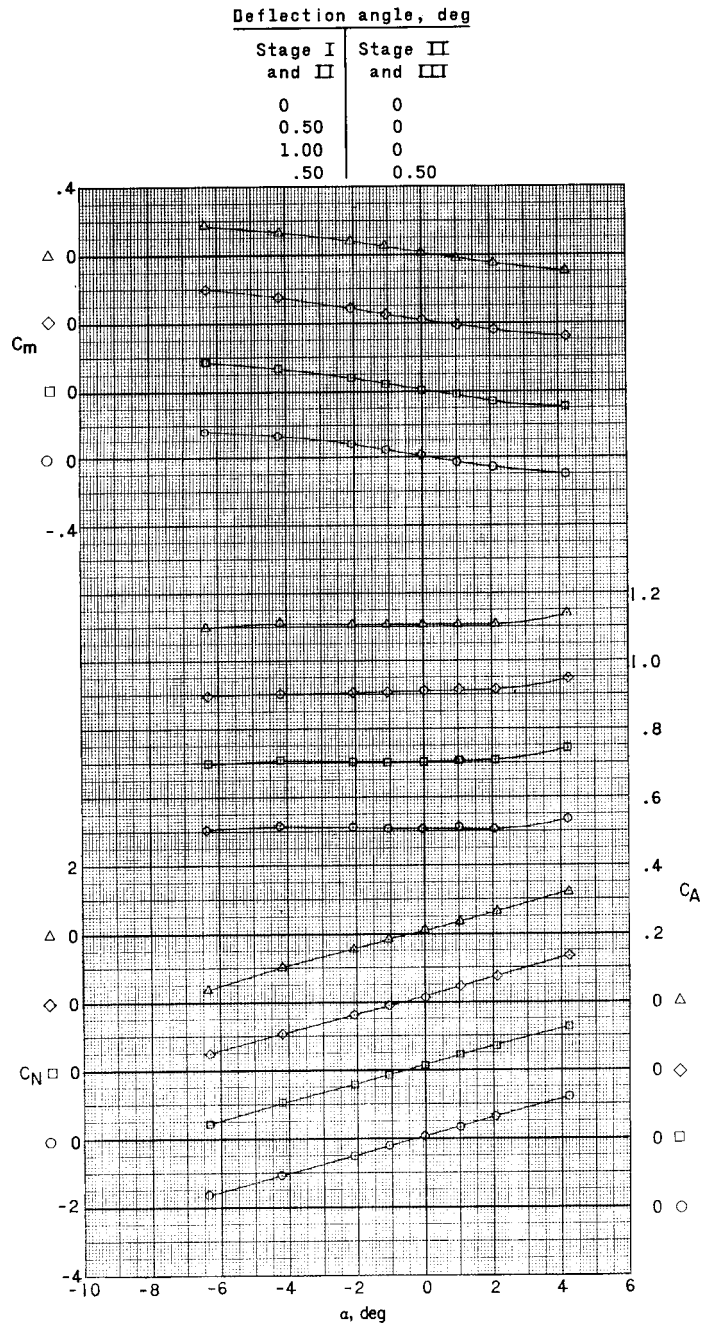
Figure 7.- Continued.

CONFIDENTIAL



(c) $M = 2.54$.

Figure 7.- Continued.



(d) $M = 2.87$.

Figure 7.- Concluded.

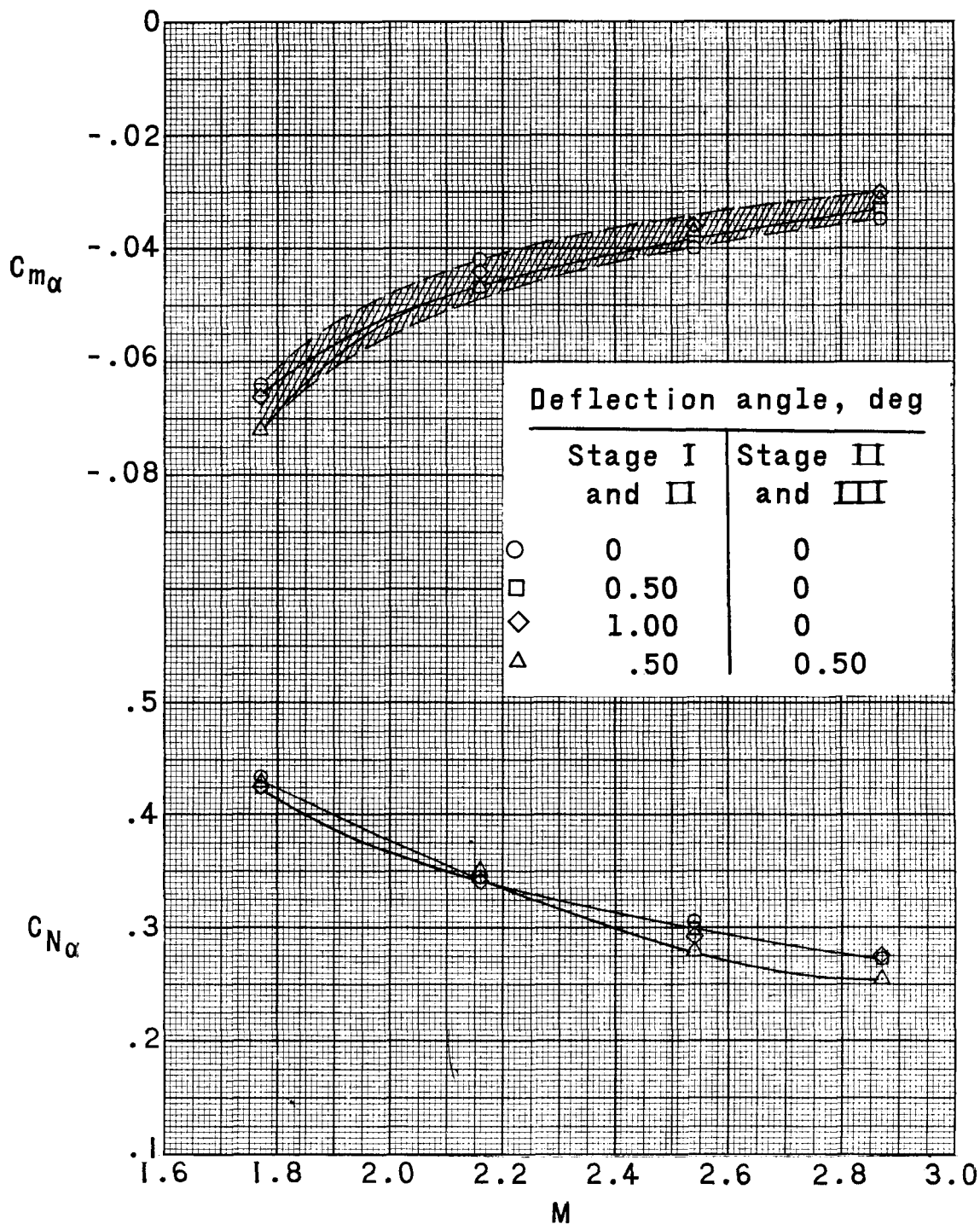
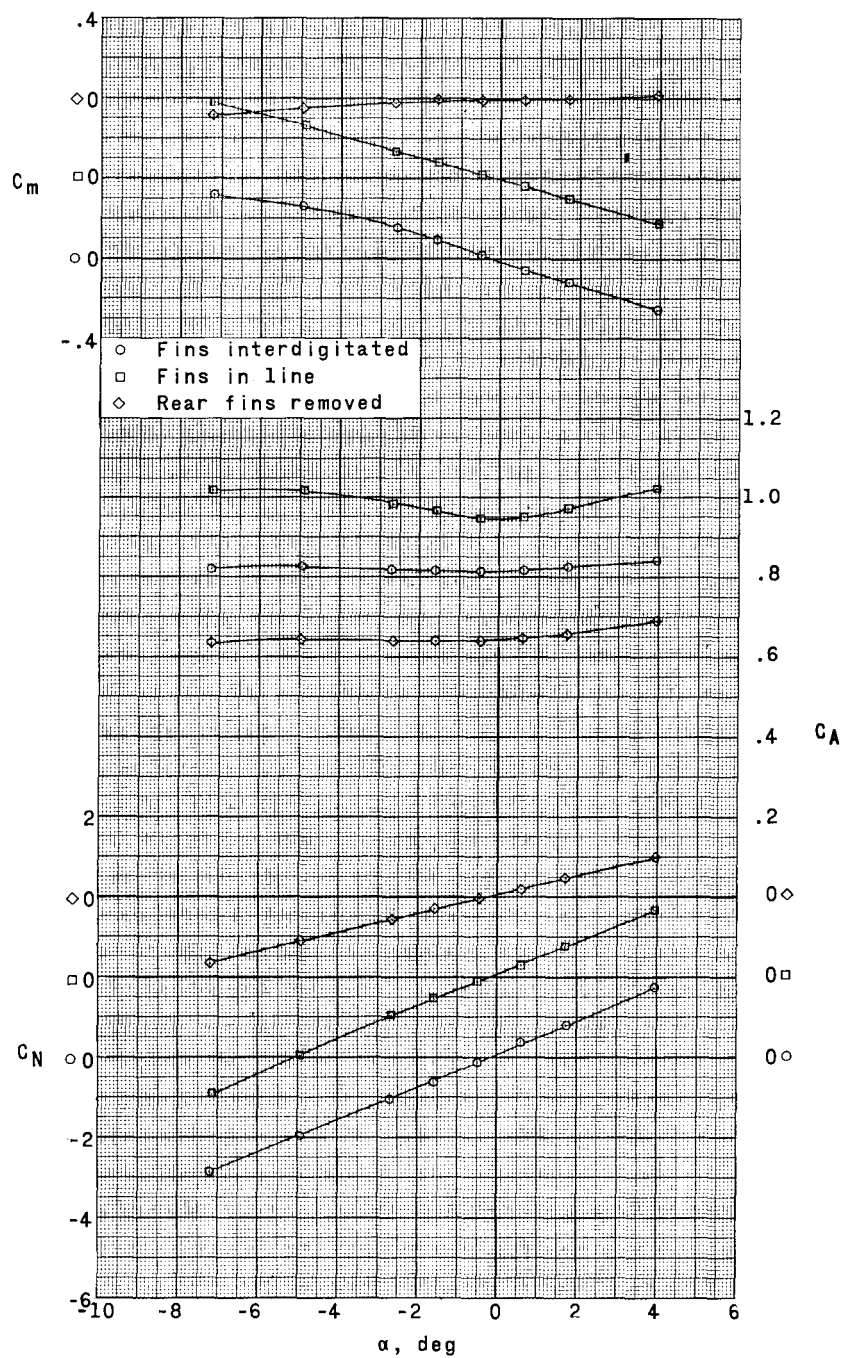


Figure 8.- Summary of longitudinal stability characteristics of body deflection.

031412501040

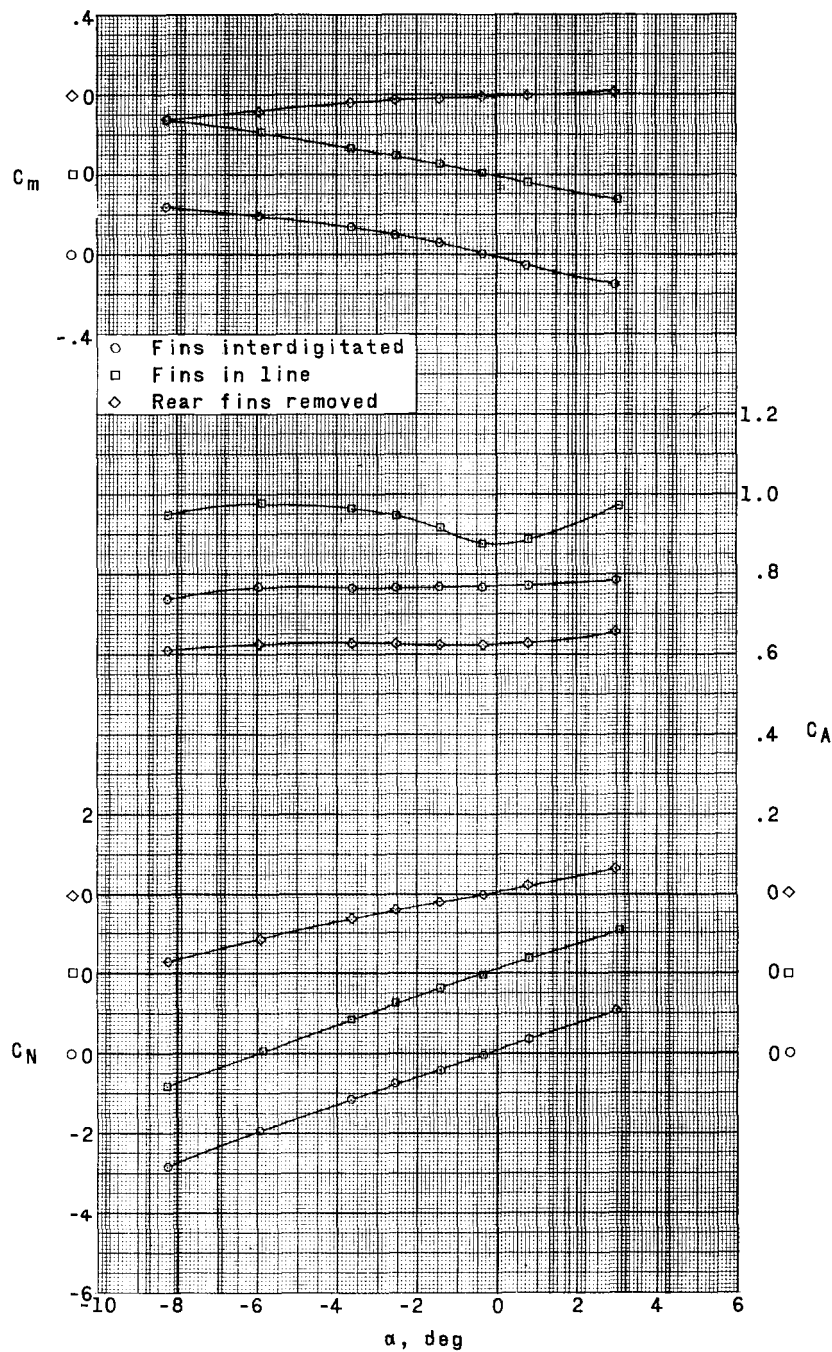
CONFIDENTIAL



(a) $M = 1.77$.

Figure 9.- Effect of relative fin alignment on aerodynamic characteristics in pitch.

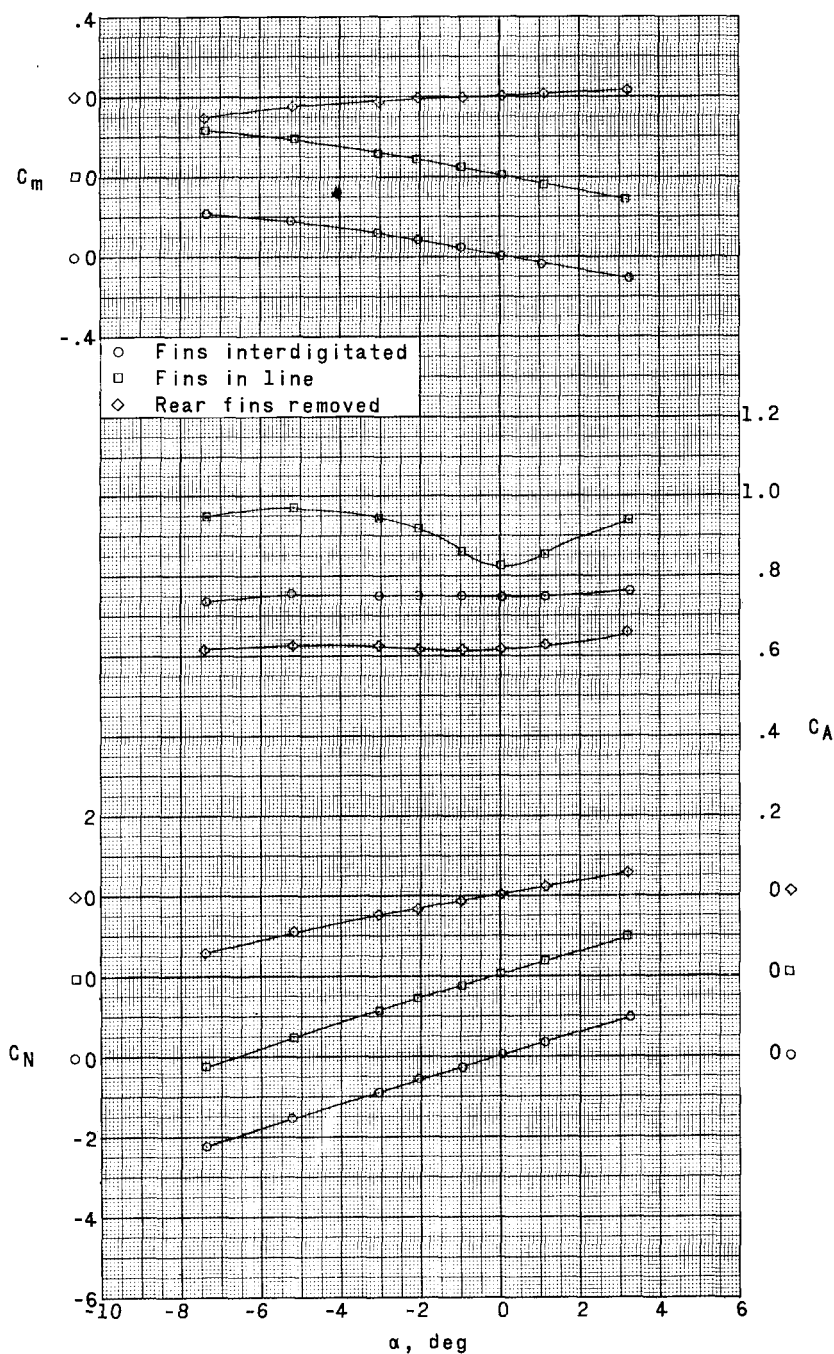
CONFIDENTIAL



(b) $M = 2.16$.

Figure 9.- Continued.

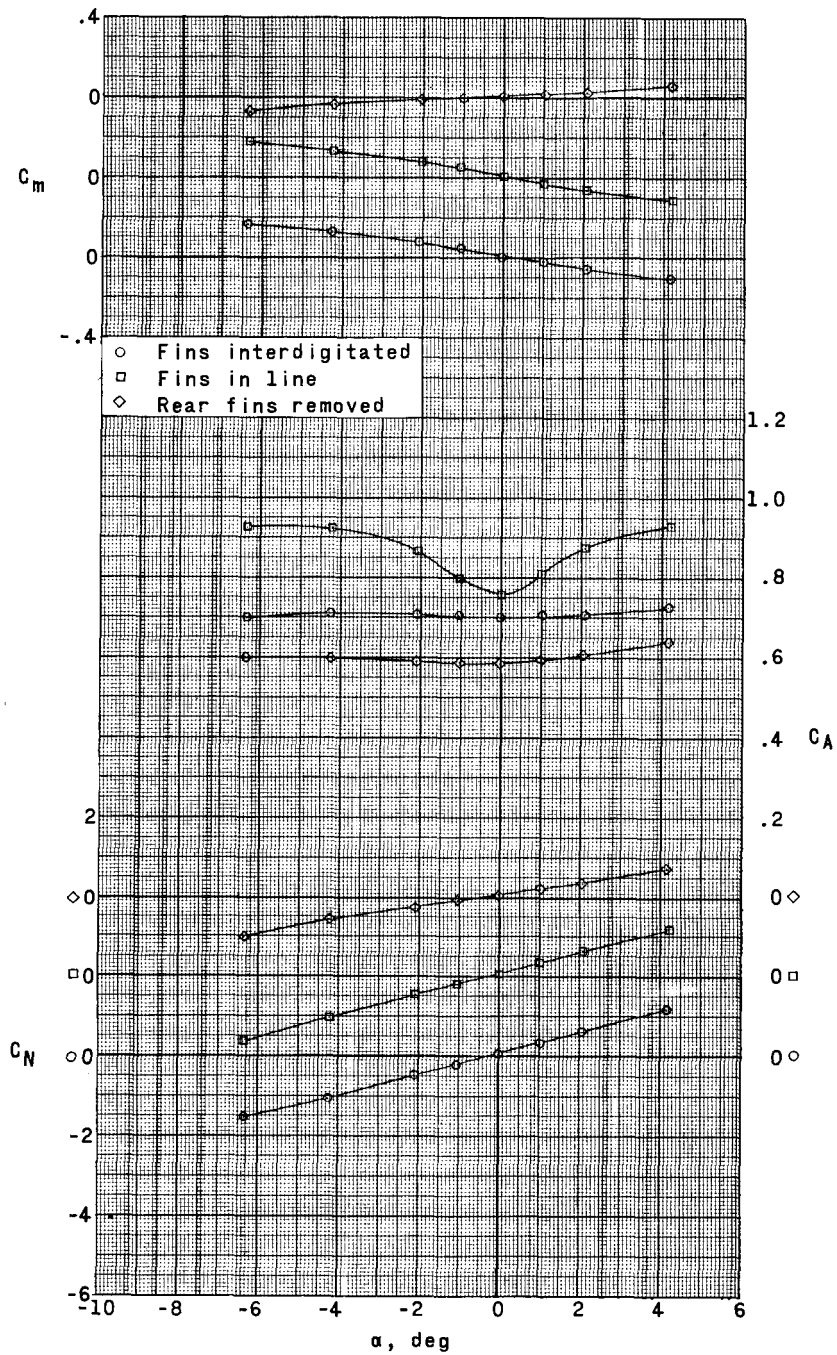
CONFIDENTIAL



(c) $M = 2.54$.

Figure 9.- Continued.

CONFIDENTIAL



(d) $M = 2.87$.

Figure 9.- Concluded.

031713 39 1040

CONFIDENTIAL

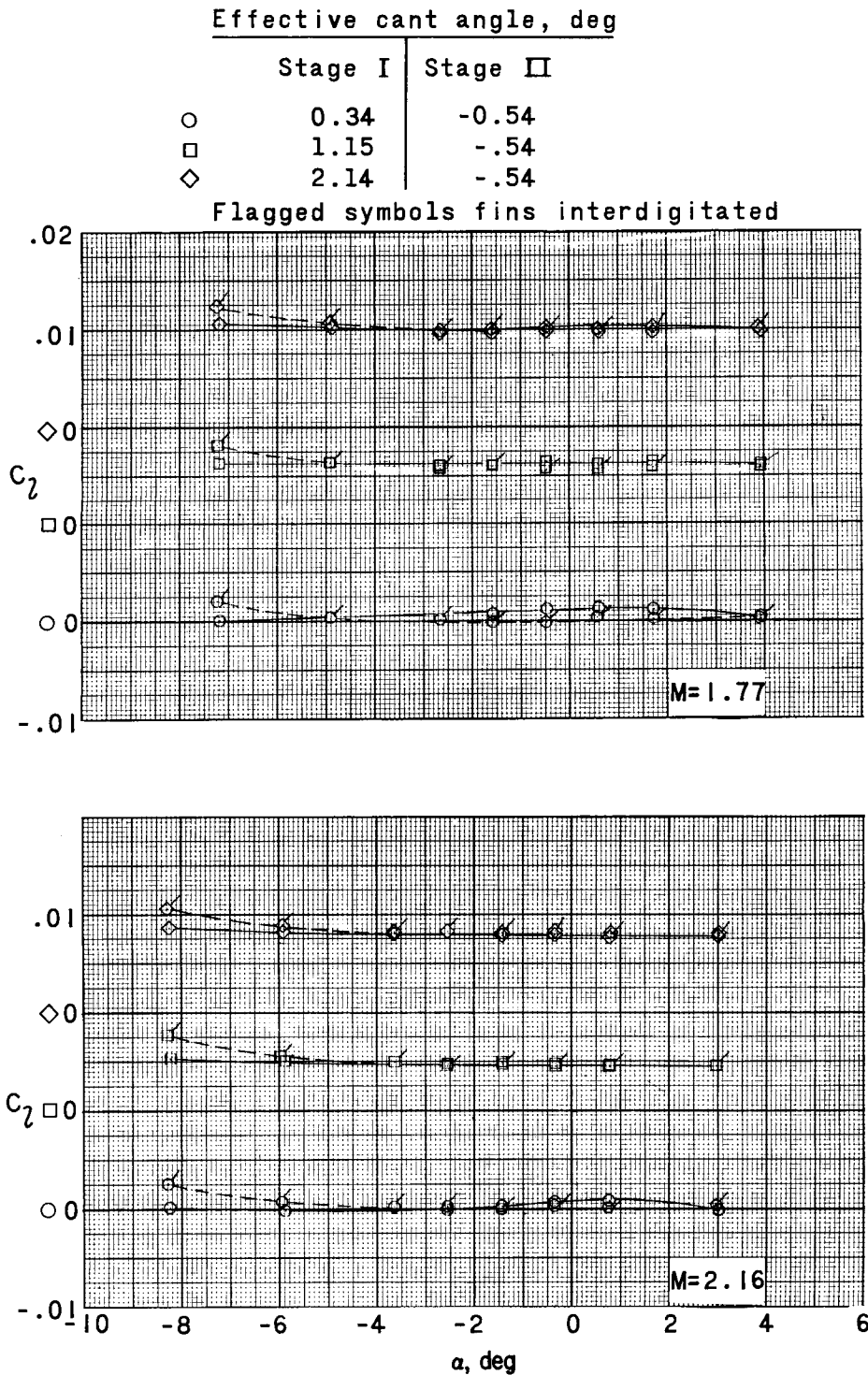
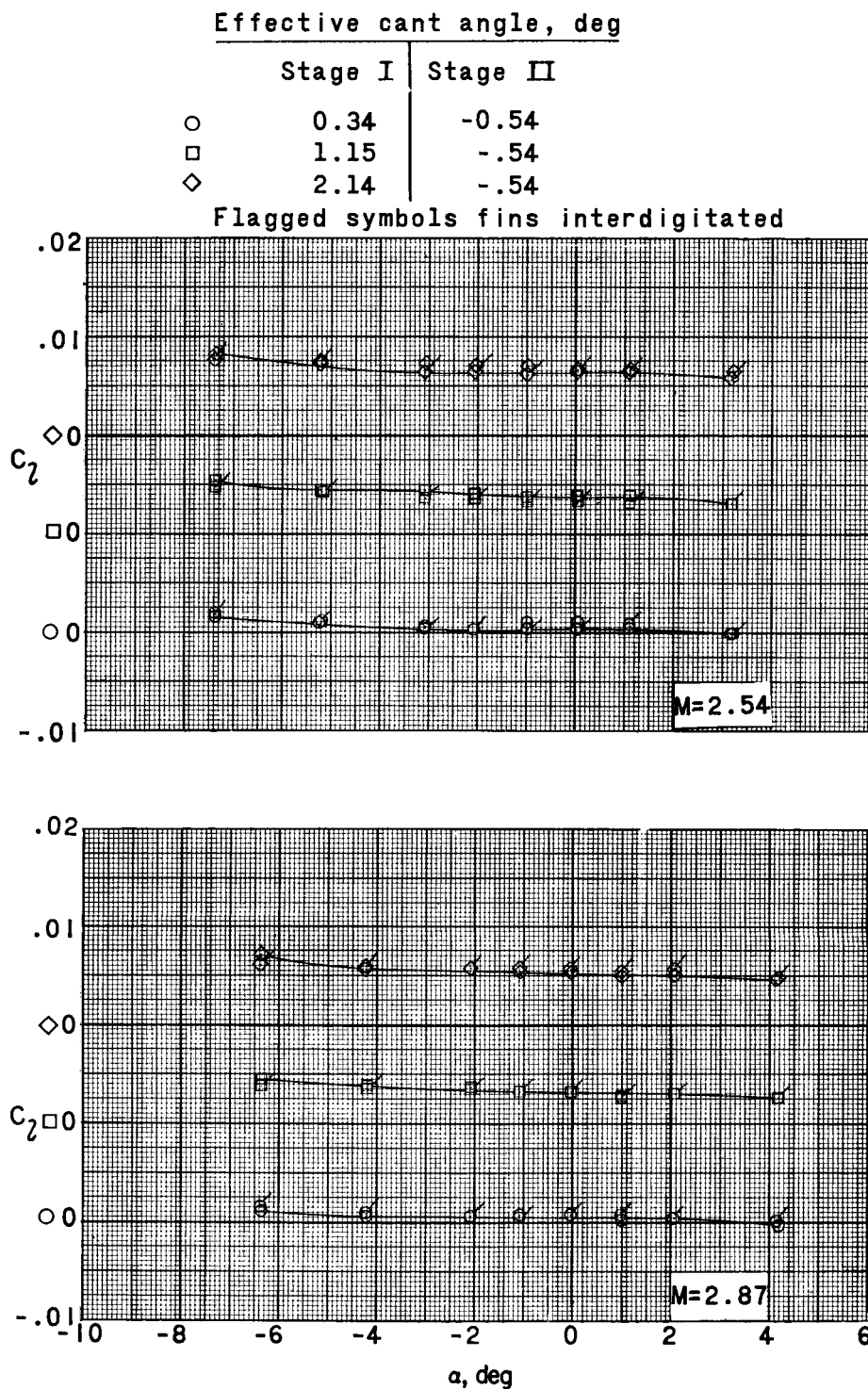


Figure 10.- Effect of stage I fin cant on rolling-moment coefficient.

CONFIDENTIAL



031713 30 JANU

CONFIDENTIAL

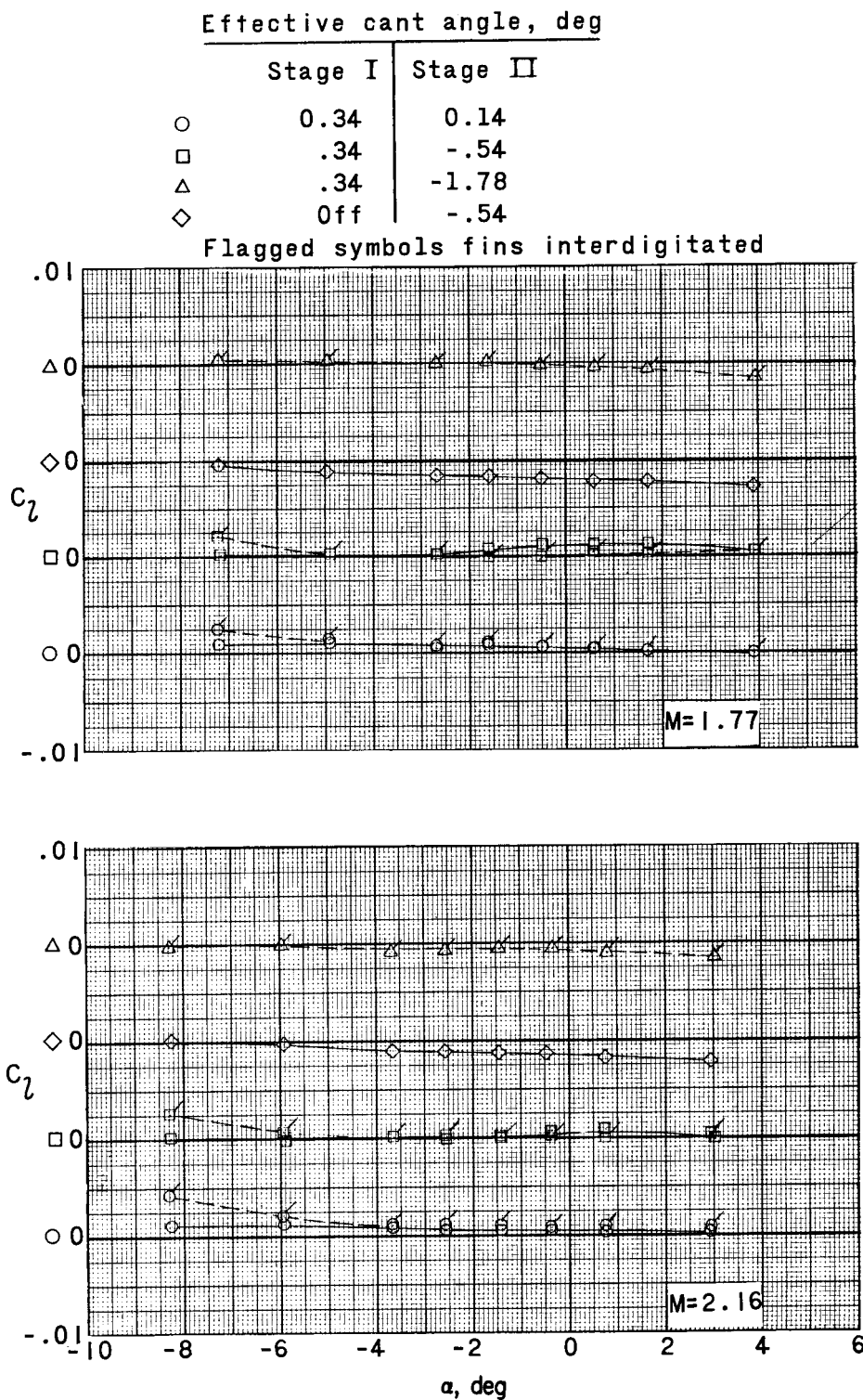


Figure 11.- Effect of stage II fin cant on rolling-moment coefficient.

CONFIDENTIAL

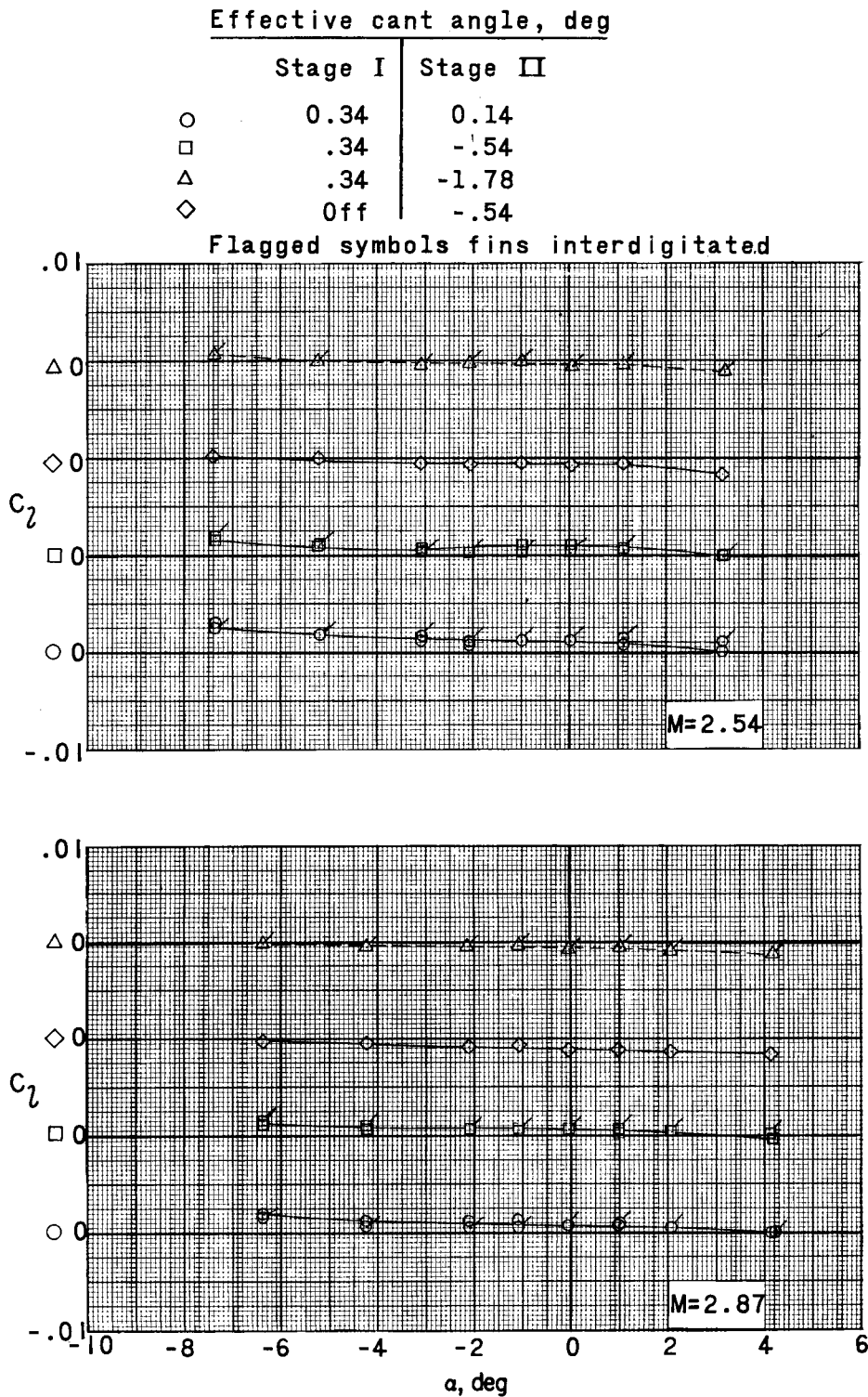


Figure 11.- Concluded.

03171229 JOMU